Quadrature imbalance compensation algorithm based on statistical properties of signals in CO-QPSK system

Yaojun Qiao (乔耀军)*, Yanfei Xu (徐艳飞), Lujiao Li (李炉焦), and Yuefeng Ji (纪越峰)

State Key Laboratory of Information Photonics and Optical Communications, Beijing University of Posts and Telecommunications, Beijing 100876, China

**Corresponding author: qiao@bupt.edu.cn*

Received April 10, 2012; accepted July 10, 2012; posted online October 16, 2012

We propose a blind quadrature imbalance (QI) compensation algorithm based on the statistical properties of I and Q signals in a receiver. The algorithm estimates the QI parameters of a receiver by calculating the mean, variance, and correlation coefficient of I and Q components. Then, the estimated imbalance parameters are adopted to compensate for the QI in the receiver. Simulation results show that the Q factor is considerably optimized by the application of the QI compensation algorithm in an 80-Gb/s Pol-Mux coherent optical quadrature phase-shift keying (CO-QPSK) system. Compared with conventional algorithms, the proposed algorithm exhibits better performance when the phase deviation from QI exceeds $\pm 15^\circ$.

OCIS codes: 060.0060, 060.1660, 060.2330, 070.6020.
doi: 10.3788/COL201210.120601.

Coherent detection technology for long-haul and high-speed transmission has recently attracted considerable attention because such technology presents high receiver sensitivity[1] and spectral efficiency[2]. Coherent detection can obtain complete optical field information, including that amplitude and phase, thereby enabling the compensation of dispersion and nonlinearity in the electrical domain by digital signal processing (DSP)[3]. Multilevel optical modulation formats with high spectral efficiency and robust resistance to linear impairments have also been extensively investigated[4]. Quadrature phase-shift keying (QPSK) with a coherent detection scheme is widely used in high-speed optical communications[5−7], and is one of the most promising modulation formats because of its superior transmission characteristics[8].

Ideally, the amplitudes of the I/Q channel signals of a receiver are equal, and the phase difference between channels is 90° in a QPSK system with a coherent receiver. However, an imperfect optical 90° hybrid may cause amplitude and phase imbalances[9]. This effect is called quadrature imbalance (QI)[10]. QI affects the performance of all subsequent DSP algorithms in a receiver and diminishes the performance of a QPSK system[11]. To correct QI, many compensation algorithms have been proposed: in Ref. [9], the Gram–Schmidt orthogonalization procedure (GSOP) was used to correct non-orthogonality; in Ref. [11], a QI compensation scheme based on the constant modulus algorithm was proposed; in Ref. [12], the least-squares algorithm was applied to fit constellation to an ellipse, after which the ellipse parameters were extracted and then used to estimate the amplitude and phase imbalance parameters. Real-time QI compensation has also been recently reported[13]. In this letter, we propose a blind QI compensation algorithm based on the statistical properties of received signals. The algorithm calculates the mean, variance, and correlation coefficient of I and Q components. Then, the calculated parameters are applied to estimate imbalance parameters. With given amplitude and phase imbalance parameters, QI compensation is performed. The proposed algorithm is tested by simulation in an 80-Gb/s back-to-back (B2B) coherent optical (CO)-QPSK system. The performance of the proposed algorithm, combined with the phase estimation (PE) algorithm[14], is also examined. Simulation results show that the compensation algorithm increases the Q factor of the system with QI to a value observed in a system with quadrature balance in an 80-Gb/s CO-QPSK system.

For simplicity, we assume that the I branch is ideal, and that imbalance is introduced only in the Q branch. We also assume that the phase difference between a carrier and local oscillators is zero. Figure 1 shows the schematic of the proposed QI compensation algorithm.

In Fig. 1, $s(t)$ denotes the original signal without QI, $s(t) = s_{\rm I}(t) + {\rm j}s_{\rm Q}(t)$; $x(t)$ represents the received signal with QI, $x(t) = x_{\rm I}(t) + {\rm j}x_{\rm Q}(t)$; and $y(t)$ is the equalized signal, $y(t) = y_{\rm I}(t) + {\rm j}y_{\rm Q}(t)$.

The relationship between $x(t)$ and $s(t)$ is expressed as[15]

$$x(t) = K_1 s(t) + K_2 s^*(t), \tag{1}$$

where * denotes complex conjugation, and imbalance factors K_1 and K_2 can be expressed as

$$\begin{cases} K_1 = \dfrac{1 + g{\rm e}^{-{\rm j}\delta}}{2} \\ K_2 = \dfrac{1 - g{\rm e}^{{\rm j}\delta}}{2} \end{cases}, \tag{2}$$

where g and δ are the amplitude and phase imbalance factors, respectively. When the I and Q branches perfectly match (that is, g=1 and δ=0), we can obtain $K_1 = 1$ and $K_2 = 0$. Using Eq. (2) and splitting Eq. (1) into real and imaginary parts, we can rewrite Eq. (1) as

$$\begin{cases} x_{\rm I}(t) = s_{\rm I}(t) \\ x_{\rm Q}(t) = g\cos(\delta)s_{\rm Q}(t) - g\sin(\delta)s_{\rm I}(t) \end{cases}. \tag{3}$$

In matrix formulation, Eq. (3) can be rewritten as

$$\begin{bmatrix} x_{\rm I}(t) \\ x_{\rm Q}(t) \end{bmatrix} = \begin{bmatrix} 1 & 0 \\ -g\sin(\delta) & g\cos(\delta) \end{bmatrix} \begin{bmatrix} s_{\rm I}(t) \\ s_{\rm Q}(t) \end{bmatrix} = A \begin{bmatrix} s_{\rm I}(t) \\ s_{\rm Q}(t) \end{bmatrix}, \tag{4}$$

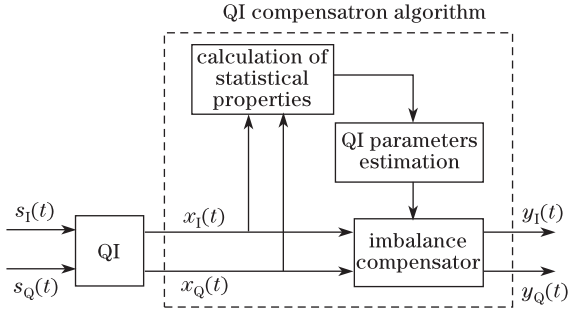

Fig. 1. Schematic of the QI compensation algorithm.

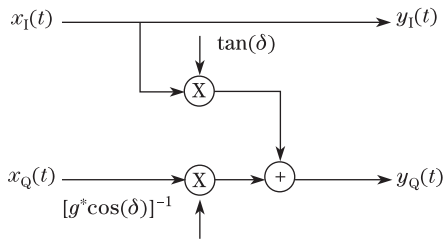

Fig. 2. Imbalance compensator of the QI compensation algorithm.

where

$$\boldsymbol{A} = \begin{bmatrix} 1 & 0 \\ -g\sin(\delta) & g\cos(\delta) \end{bmatrix}. \tag{5}$$

Thus, we can obtain equalized signal $y(t)$ by premultiplying Eq. (4) by the inverse matrix of $\boldsymbol{A}$:

$$\begin{bmatrix} y_I(t) \\ y_Q(t) \end{bmatrix} = \boldsymbol{A}^{-1} \begin{bmatrix} x_I(t) \\ x_Q(t) \end{bmatrix} = \begin{bmatrix} 1 & 0 \\ \tan(\delta) & [g\cos(\delta)]^{-1} \end{bmatrix} \begin{bmatrix} x_I(t) \\ x_Q(t) \end{bmatrix}. \tag{6}$$

That is, $y_Q(t) = \tan(\delta)x_I(t) + [g\cos(\delta)]^{-1}x_Q(t)$, $y_I(t) = x_I(t)$. Then, we can obtain the imbalance compensator of Fig. 1, as illustrated in Fig. 2. Hence, we first calculate g, $\tan(\delta)$, and $\cos(\delta)$ to obtain $y(t)$.

We assume that s_I and s_Q are i.i.d. random processes with mean u and variance σ^2. The means and variances of x_I and x_Q can be expressed as[16]

$$\begin{cases} E(x_I) = u \\ var(x_I) = \sigma^2 \end{cases} \tag{7}$$

Thus,

$$\begin{cases} E(x_Q) = gu[\cos(\delta) - \sin(\delta)] \\ \mathrm{var}(x_Q) = g^2\sigma^2 \end{cases}. \tag{8}$$

Using Eqs. (7) and (8), we can obtain the amplitude imbalance factor

$$g = \sqrt{\mathrm{var}(x_Q)/\mathrm{var}(x_I)}. \tag{9}$$

To estimate parameter δ, we determine the correlation coefficient of x_I and x_Q with

$$\rho_{x_I x_Q} = E\left[\frac{x_I - E(x_I)}{\sigma_{x_I}} \cdot \frac{x_Q - E(x_Q)}{\sigma_{x_Q}}\right]. \tag{10}$$

According to Eqs. (7) and (8), we can obtain $\sigma_{x_I} = \sigma$, $\sigma_{x_Q} = g\sigma$. Substituting σ_{x_I} and σ_{x_Q} into Eq. (10) and performing mathematical manipulations yield

$$\rho_{x_I x_Q} = \frac{1}{g\sigma^2}[E(x_I x_Q) - E(x_I)E(x_Q)]. \tag{11}$$

Using Eqs. (3), (7), and (8), as well as the statistical independence between s_I and s_Q as bases, we can rewrite Eq. (11) as

$$\begin{aligned} \rho_{x_I x_Q} &= \frac{1}{g\sigma^2}\{E\{s_I[g\cos(\delta)s_Q - g\sin(\delta)s_I] - gu^2[\cos(\delta) - \sin(\delta)]\} \\ &= \frac{1}{\sigma^2}\left\{\cos(\delta)E(s_I)E(s_Q) - \sin(\delta)E(s_I^2) - u^2[\cos(\delta) - \sin(\delta)]\right\} \\ &= \frac{1}{\sigma^2}\{[u^2\cos(\delta) - \sin(\delta)(u^2 + \sigma^2) - u^2[\cos(\delta) - \sin(\delta)]\} \\ &= \frac{1}{\sigma^2} \times [-\sigma^2\sin(\delta)] = -\sin(\delta). \end{aligned} \tag{12}$$

With Eq. (12), parameter δ can be easily estimated as

$$\delta = -\mathrm{arc}\sin(\rho_{x_I x_Q}). \tag{13}$$

Thus, we first calculate the statistical properties of the received signals, and then estimate the amplitude and phase imbalance parameters. Equation (6) or Fig. 2 is subsequently applied to compensate for QI.

To test the proposed QI compensation algorithm, numerical simulations are performed in the 80-Gb/s Pol-Mux B2B CO-QPSK system. VPI Transmission Maker 7.6 is used for the simulations. The schematic of this system is shown in Fig. 3.

In the transmitter, the QPSK signal is obtained using an integrated LiNbO3 Mach–Zehnder modulator (MZM), which is driven by 20-Gb/s I and Q drive signals. Push-pull operation is adopted on both the sub-MZMs of the nested MZM. The external cavity laser is located at 1550 nm, with the linewidth set at 100 kHz. To achieve polarization multiplexing, the same configurations of the dual-parallel MZM described above are implemented in Pol X and Pol Y. At the end of the Pol-Mux transmitter, a polarization beam combiner (PBC) is used to converge the separate polarizations that form the 80-Gb/s Pol-Mux QPSK signal.

At the receiver, the Pol-Mux signal is first sent to a polarization beam splitter (PBS) to separate Pol X and Pol Y. Then, the polarization demultiplexed QPSK signals are sent to corresponding DSP unit beats with the local oscillator (LO) signal in a 90° optical hybrid to obtain the I and Q components of the signal. The LO frequency offset is set at 50 MHz. The 90° optical hybrid is followed by two balanced photodiodes (PDs). An analog-to-digital converter (ADC) with a sampling rate fixed at 80 GSa/s is used to sample each signal for offline processing (4 rounds of up-sampling). QI, which results from the imperfection of the optical 90° hybrid, is then compensated. After QI compensation, PE is adopted when the phase difference between the transmitter and the local oscillator is nonzero. Finally, the bit error rate (BER) is estimated using the Monte Carlo method over 217 bits. In the simulations, we set the optical signal-to-noise ratio (SNR) to 14 dB.

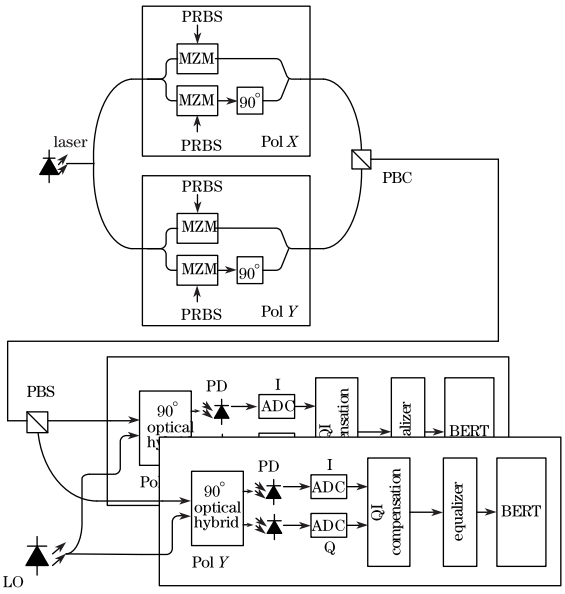

Fig. 3. Simulation configuration of the 80Gb/s Pol-Mux CO-QPSK system.

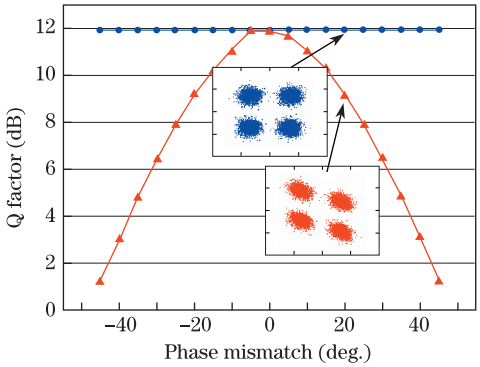

Fig. 4. (Color online) Q factor versus phase mismatch. Insets show the constellation diagrams of the received signals for a phase mismatch of 20° with (blue) and without (red) QI compensation.

The validity of the QI compensation algorithm is first tested. We set the phase mismatch of the 90° optical hybrid to 30° and the 3-dB coupler coupling coefficients to +40% of their nominal value (i.e., coupling coefficient is 0.7). The Q branch-to-I branch amplitude ratio is $\sqrt{0.7/(1-0.7)}$=1.528. The g and δ obtained by simulation are 1.525 and 30.2°, respectively, indicating good agreement between simulation and theory.

Phase mismatch is introduced in the phase shifter of the 90° optical hybrid, and only its effect on the performance of the QPSK system is investigated. Figure 4 shows the Q factor as a function of phase mismatch. The Q factor significantly decreases with increasing phase mismatch when no QI compensation is performed. With QI compensation, the performance deterioration caused by different phase mismatch degrees is eliminated and the Q factor increases to 11.94 dB, a value identical to that derived in the system without QI. The lower inset in Fig. 4 shows the received signal for a phase mismatch of 20° in the 90° optical hybrid. This mismatch causes a skew in the constellation diagram.

After applying the QI compensation algorithm to compensate for non-orthogonality, the signal is recovered in the form of four orthogonal phase states (upper inset, Fig. 4).

In a CO-QPSK system, the I and Q branches are separately received. Thus, amplitude imbalance does not affect system performance. This effect is attributed to the fact that amplitude imbalance does not influence the electrical SNR. However, when the I and Q branches are combined to perform electronic equalization, amplitude imbalance significantly affects the performance of all subsequently applied DSP algorithms, such as PE. To consider the effect of amplitude imbalance on PE in the simulation, we set the 3-dB coupler coupling coefficient to 0.7, as well as the transmitter laser and LO with a linewidth of 100 kHz and frequency offset of 50 MHz, respectively. Figure 5(a) shows the received constellation diagram without QI compensation and PE (left), with PE only (center), and with both QI compensation and PE (right).

In the presence of amplitude imbalance and phase difference between the carrier and LO, the constellation becomes elliptical (left side, Fig. 5(a)). The center of Fig. 5(a) corresponds to the output of PE when QI compensation is applied beforehand. QI prevents PE from appropriately functioning, thereby leading to distorted constellations. When QI compensation is performed before PE, the effect of QI and phase difference is effectively cancelled, and the quality of a constellation significantly improves (right side, Fig. 5(a)).

The effect of phase mismatch on PE is also investigated. The phase mismatch of the 90° optical hybrid is set to 20°, and the transmitter laser and LO are set with a linewidth of 100 kHz and a frequency offset of 50 MHz, respectively. The left side of Fig. 5(b) shows the combined effects of phase mismatch and phase difference between the carrier and LO. The constellation becomes a skew ellipse. The center of Fig. 5(b) shows a distorted constellation when only PE is applied because of the effect of phase mismatch on the implementation of the PE algorithm.

Phase mismatch causes PE to yield inaccurate results. When QI compensation is applied before PE, the signals are successfully recovered (right side, Fig. 5(b)).

Compared with universal algorithms for QI compensation (e.g., GSOP), the proposed QI compensation

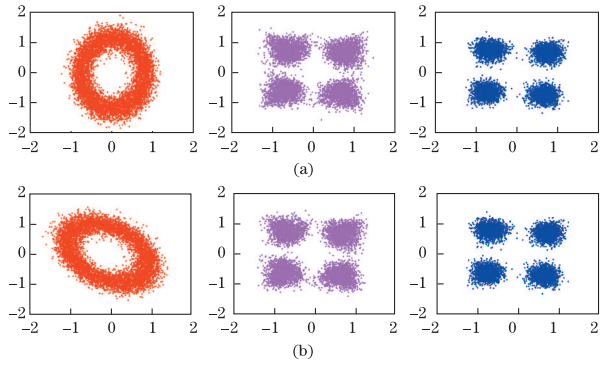

Fig. 5. Constellation diagrams of the received signals for (a) a coupling coefficient and (b) a phase mismatch of 0.7, (left) without QI compensation and PE, (central) with PE alone, and (right) with QI compensation and PE.

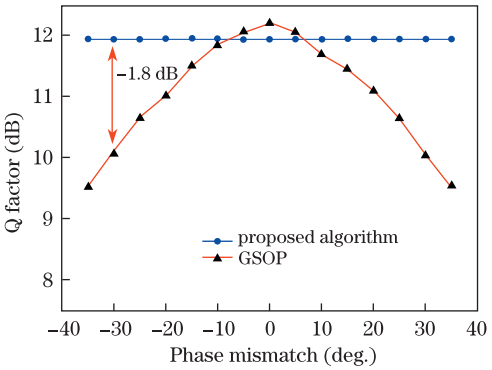

Fig. 6. Q factor versus phase mismatch versus the proposed QI compensation algorithm and the GSOP algorithm.

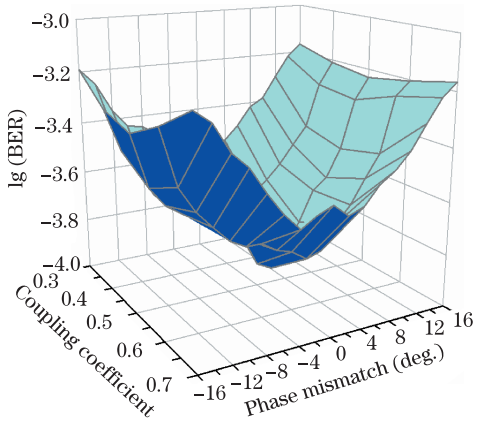

Fig. 7. BER versus various settings of phase mismatch and coupling coefficients.

algorithm exhibits better performance when phase deviation exceeds ±15° (Fig. 6). When phase mismatch reaches ±35°, a 1.8-dB superiority over conventional algorithm is achieved.

Figure 7 shows the BER as a function of various settings of the 90° optical hybrid when no QI compensation is implemented.

All deviations from the nominal settings increase the BER. Phase mismatch is the most influential defect. When the phase difference is nonzero, Eq. (3) is rewritten as

$$\begin{cases} x_{\mathrm{I}}(t) = s_{\mathrm{I}}(t)\cos(\theta) - s_{\mathrm{Q}}(t)\sin(\theta) \\ x_{\mathrm{Q}}(t) = g\cos(\delta-\theta)s_{\mathrm{Q}}(t) - g\sin(\delta-\theta)s_{\mathrm{I}}(t) \end{cases}. \quad (14)$$

Equation (14) indicates that the estimation of phase difference θ is affected by phase imbalance, thereby causing phase mismatch to have a more considerable effect on the PE algorithm than does amplitude imbalance. Compared with amplitude imbalance, phase imbalance results in greater BER fluctuation (Fig. 6). When QI compensation is performed before PE, however, QI is completely compensated and the BERs of various settings decrease to those obtained in the system without QI. That is, BER improves to the value of the ideal setting in Fig. 6 (i.e., the degree of phase mismatch is zero and the coupling coefficient is 0.5).

In conclusion, QI arises from imperfections in a coherent receiver. Its effect on the performance of optical QPSK communication systems is investigated. QI is a ubiquitous phenomenon that affects the performance of subsequently applied DSP algorithms and degrades system performance. To correct QI, we propose a blind QI compensation algorithm based on the statistical properties of received signals. Given that QI is constant during a single measurement, only a small number of received signals are required to calculate statistical properties, which leads to low complexity. The proposed QI compensation algorithm is tested by simulations in an 80-Gb/s B2B CO-QPSK system. The proposed method significantly eliminates the various imperfections caused by the receiver QI and improves system performance.

This work was supported by the National Natural Science Foundation of China (No. 60932004), the National "973" Program of China (No. 2012CB315705), and the National "863" Program of China (No. 2011AA010306).

References

1. L. G. Kazovsky, G. Kalogerakis, and W. Shaw, J. Lightwave Technol. **24,** 4876 (2006).
2. J. M. Kahn and K.-P. Ho, IEEE J. Sel. Top. Quantum Electron. **10,** 259 (2004).
3. E. Ip and J. M. Kahn, J. Lightwave Technol. **28,** 502 (2010).
4. I. Morohashi, M. Sudo, T. Sakamoto, A. Kanno, A. Chiba, J. Ichikawa, and T. Kawanishi, in *Proceedings of ECOC 2010* P3.14 (2010).
5. D. van den Borne, V. A. J. M. Sleifferet, M. S. Alfiad, S. L. Jansen, and T. Wuth, in *Proceedings of ECOC 2009* 3.4.1 (2009).
6. M. Birk, P. Gerard, R. Curto, L. E. Nelson, X. Zhou, P. Magill, T. J. Schmidt, C. Malouin, B. Zhang, E. Ibragimov, S. Khatana, M. Glavanovic, R. Lofland, R. Marcoccia, R. Saunders, G. Nicholl, M. Nowell, and F. Forghieri, J. Lightwave Technol. **29,** 417 (2011).
7. J. X. Cai, Y. Cai, C. Davidson, D. Foursa, A. Lucero, O. Sinkin, W. Patterson, A. Pilipetskii, G. Mohs, and N. S. Bergano, J. Lightwave Technol. **29,** 491 (2011).
8. Ivan P. Kaminow, T. Li, and A. Willner, *Optical Fiber Telecommunications V B: Systems and Networks* (Academic Press, New York, 2008) chap. 20.
9. I. Fatadin, D. Ives, and S. J. Savory, IEEE Photon. Technol. Lett. **20,** 1733 (2008).
10. I. Roudas, M. Sauer, J. Hurley, Y. Mauro, and S. Raghavan, in *Proceedings of LEOS 2007* MA3.4 (2007).
11. C. S. Petrou, A. Vgenis, I. Roudas, and L. Raptis, Photon. Technol. Lett. **21,** 1876 (2009).
12. C. S. Petrou, A. Vgenis, A. Kiourti, I. Roudas, J. Hurley, M. Sauer, J. Downie, Y. Mauro, and S. Raghavan, in *Proceedings of LEOS 2008* TuFF3 (2008).
13. S. Chen, A. Al Amin, and W. Shieh. in *Proceedings of OFC 2011* OWE2 (2011).
14. A. J. Viterbi and A. M. Viterbi, IEEE Trans. Inform. Theory **29,** 543 (1983).
15. M. Valkama, M. Renfors, and V. Koivunen, IEEE Trans. Signal Process. **49,** 2335 (2001).
16. A. Papoulis, *Probability, Random Variables, and Stochastic Processes* (McGraw-Hill, New York, 1991).